JOURNAL OF MATERIALS SCIENCE 28 (1993) 389–393

Application of Mössbauer spectroscopy to study the formation of iron pyrite thin films

I. J. FERRER, C. DE LAS HERAS, N. MENÉNDEZ*, J. TORNERO,* C. SÁNCHEZ
*Departamento de Física Aplicada C-IV and **Departamento de Química Física Aplicada C-II, U.A.M. Cantoblanco, 28049 Madrid, Spain*

Mössbauer spectroscopy has been used to analyse FeS_2 thin films obtained by sulphidation of ^{57}Fe evaporated layers. Complementary characterization of the films has been carried out by X-ray diffraction and optical absorption measurements. It is concluded that the two processes (formation and crystallization of FeS_2) which lead to polycrystalline FeS_2 films are strongly influenced by the temperature at which sulphidation is accomplished. The composition of the films drastically changes at temperatures which depend on the thickness of the Fe film to be sulphidated, and their crystallization seems to show a critical temperature at which the crystallization process is severely altered. Optical properties of the pyrite films seem to depend strongly on their stoichiometry.

1. Introduction

Recently, interest in the preparation of iron pyrite thin films has grown [1–3] due to the properties which make pyrite applicable to solar energy conversion cells [4, 5]. Some of the preparation methods of FeS_2 thin films include the sulphidation of oxides [6], pyrite or pyrrhotite [7] and iron films [8, 9].

In our previous work [9, 10] pyrite thin films were analysed by energy-dispersive analysis by X-ray (EDAX) and the ratio S/Fe was determined as a function of the sulphidation temperature at different sulphur pressures. However, EDAX is mainly a surface technique and no guarantee is offered that the values of the S/Fe ratio correspond to the whole of the film thickness. To face this problem we have selected ^{57}Fe Mössbauer spectroscopy as a direct and non-destructive technique for identifying and determining the relative amounts of Fe compounds present in a variety of different phases [11, 12]. Mössbauer spectra of thermally evaporated pyrite thin films have been previously used [13, 14] to determine the nature of the films. However, in this work the Mössbauer effect is used not only qualitatively, but also as a quantitative tool to analyse the FeS_2 films obtained by sulphidation of ^{57}Fe thin films. In order to complete the characterization of the sulphidated films we have also obtained their X-ray diffraction (XRD) and optical absorption spectra which, at the same time, allow us to compare the present results with those from the sulphidation of natural Fe [9, 10].

2. Experimental procedure

^{57}Fe films were thermally evaporated on glass substrates from a very small ingot of ^{57}Fe (95.2%) enriched in a Purex alumina crucible. Each one of the Fe films was annealed in a vacuum-sealed glass ampoule for about 20 h in a sulphur atmosphere. Annealing temperatures for the different films ranged from 150 to 500 °C and the sulphur pressure was in all cases 600 torr. The annealing procedure has been described elsewhere [9]. We prepared two sets of FeS_2 films: one of them with thicknesses of 0.3–0.5 μm (TH series) and the other one, obtained only at the lower sulphidation temperatures ($\leqq 350$ °C), of about 2 μm (GR series).

Mössbauer spectra were recorded at room temperature in transmission geometry by using a 50 mCi source of ^{57}Co in an Rh matrix. The constant-acceleration spectrometer, velocity calibration and computation procedures have been previously described [15]. The maximum statistical error in the experimental points was 0.1% and the sample thickness were 0.22, 0.55 and 1.46 mg cm^{-2} of ^{57}Fe for films 0.3, 0.5 and 2 μm thick, respectively. The reproducibility of the parameters was $\pm$ 0.005 and $\pm$ 0.01 mm s^{-1} for δ and ΔQ, respectively.

XRD patterns were taken in a Siemens D-500 X-ray diffractometer with CuK_α radiation. Optical absorption spectra at room temperature, corrected for the glass substrate, were recorded using a Cary model 2415 double-beam spectrophotometer. Film thicknesses were measured with a Sloan Dektak IIA with an accuracy of $\pm$ 10 nm.

3. Results and discussion

3.1. XRD patterns

Fig. 1 shows the XRD patterns of the sulphidated ^{57}Fe films of the TH series at different sulphidation temperatures ($T > 300$ °C). All the characteristic peaks of iron pyrite appear in the diffractograms. At some sulphidation temperatures (400 and 450 °C) some peaks (shaded in the figure) due to crystallized sulphur are also present. Other very small non-identified peaks (indicated with an asterisk in the figure) can be seen at 400 °C. At annealing temperatures below 300 °C all

0022–2461

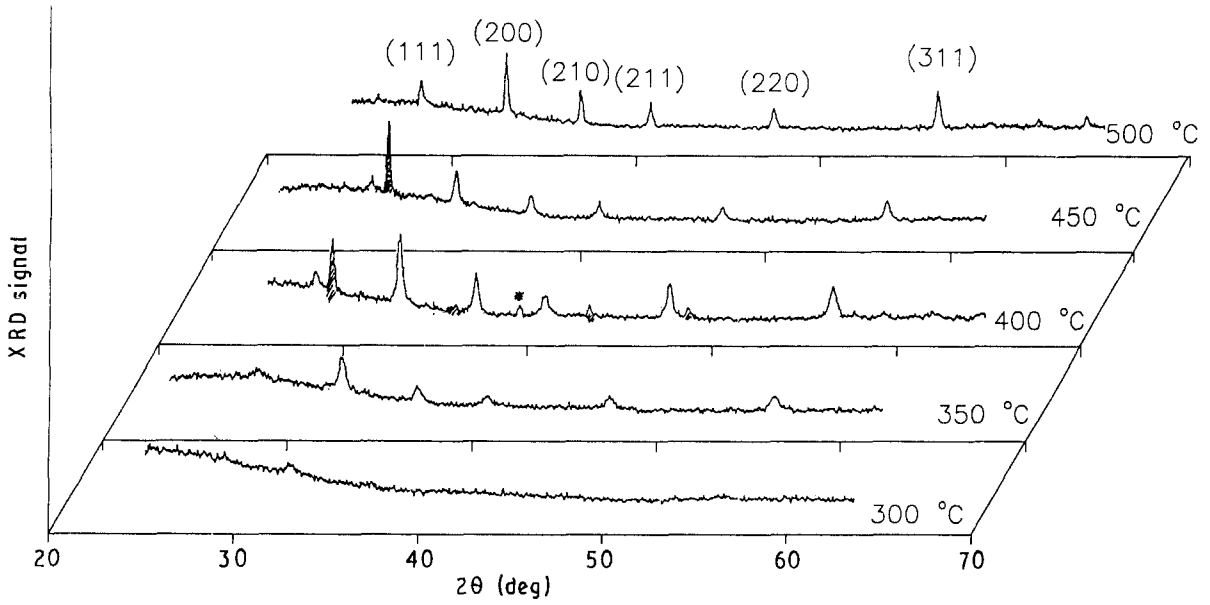

Figure 1 XRD patterns of ^{57}Fe TH films sulphidated at different temperatures (shaded peaks correspond to monoclinic sulphur, (*) denotes unidentified peak). At temperatures lower than 300 °C the XRD patterns appear to be flat.

the films give a flat X-ray spectrum reflecting their insufficient crystallization.

Diffraction peak intensities change with the sulphidation temperature in a characteristic way as shown in Fig. 2, where the intensities of the (2 0 0) and (3 1 1) peaks are plotted. A maximum of the intensity appears at ≈ 400 °C which reflects a better crystallization of the films at this temperature, in agreement with results obtained with natural Fe [9]. As deduced from the data in Fig. 2 and those published elsewhere [9], the maximum in the intensity of XRD peaks will be obtained at different sulphidation temperatures (between 350 and 400 °C) depending on the relation of the sulphur pressure to the Fe film mass to be sulphidated. At temperatures $T \geqq 450$ °C the crystallization habit of the films changes and some inhomogeneities appear. Therefore, no comparison of the properties of the films prepared at these higher temperatures with those at the lower temperatures can be done. XRD patterns of the GR series films were also obtained. Those corresponding to 300, 325 and 350 °C were identical to the ones shown in Fig. 1 and those corresponding to the lower temperatures (< 300 °C) had no structure. This behaviour was parallel to that shown by the TH films.

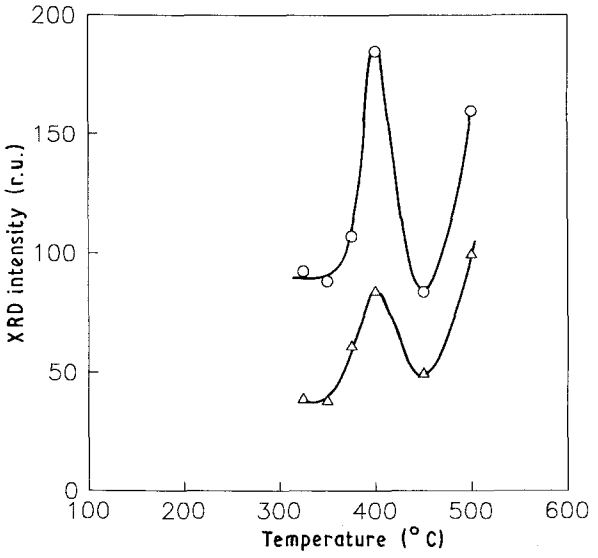

Figure 2 (○) (2 0 0) and (△) (3 1 1) XRD peak intensities from the patterns of Fig. 1 versus sulphidation temperature.

3.2. Mössbauer spectra

Mössbauer spectra of the sulphidated films were obtained and some of them are shown in Figs 3 and 4. Spectra corresponding to films sulphidated at other temperatures are not shown for the sake of clarity. At the higher temperatures the quadrupole doublet corresponding to FeS_2 can be clearly identified. However, at the lower annealing temperatures ($T = 150$ °C for TH films and $T \leqq 250$ °C for GR series) not only the two lines corresponding to pyrite are observed but a contribution of metallic iron also appears. From the relative areas of both contributions the proportions of Fe and FeS_2 can be estimated. So, in the film of the TH series sulphidated at 150 °C, 86% is FeS_2, the remaining 14% being metallic iron. The proportions of Fe and FeS_2 are very similar in GR films sulphidated at 200 and 250 °C (about 78% Fe and 22% FeS_2) while at 300 °C metallic iron is not detected. We must emphasize the drastic change of composition of the films at certain temperatures (from 250 to 300 °C and between 150 and 200 °C for the GR and TH samples, respectively), higher for the thicker films. All these data suggest that sulphur diffusion through the Fe films determines their final composition and that Fe is turned to FeS_2 at an annealing temperature which depends on the thickness of the Fe film. On the other hand, one must conclude also that a sulphur gradient between the surface and the substrate must exist in the films.

Finally, Mössbauer parameters (isomer shift, δ, and quadrupole splitting, ΔQ) obtained from the spectra

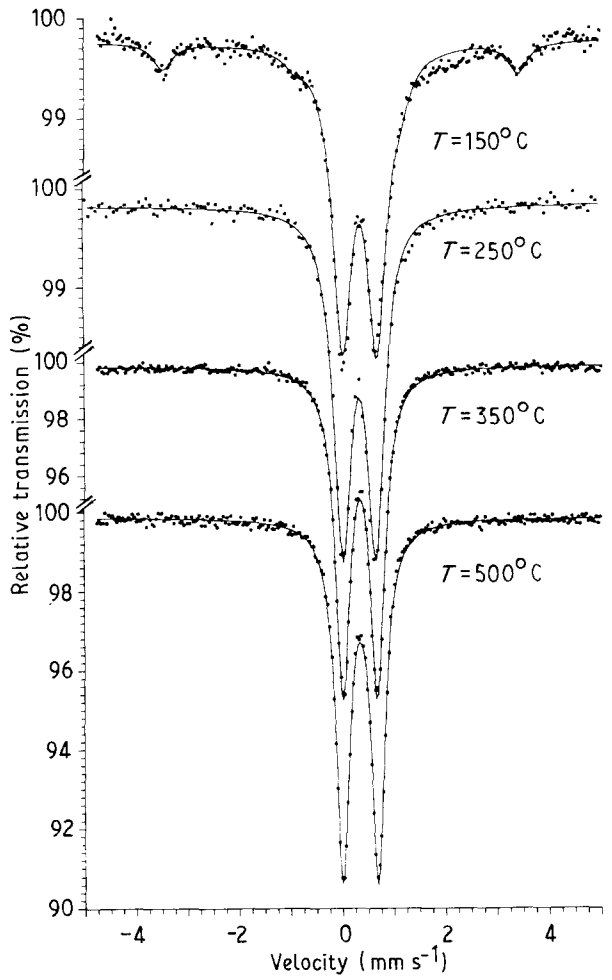

Figure 3 Mössbauer spectra obtained at room temperature of ^{57}Fe films (TH series) sulphidated at different temperatures.

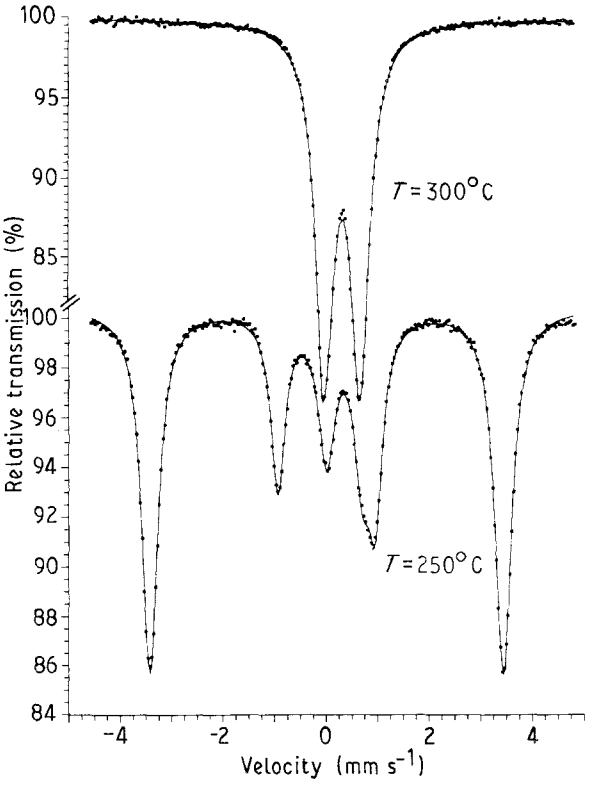

Figure 4 Mössbauer spectra obtained at room temperature of ^{57}Fe films (GR series) sulphidated at different temperatures.

confirm what has been said before about the nature of the films. They are plotted as a function of the sulphidation temperature in Fig. 5. The spread of these parameters at $T < 300\,^{\circ}C$ can be basically attributed to differences in chemical composition [11], i.e. to the presence of Fe, although differences in texture, morphology and grain size must also be kept in mind. At $T > 300\,^{\circ}C$ the values of the parameters obtained correspond fairly well to those of pure specimens of pyrite ($\delta = 0.315\ mm\,s^{-1}$, $\Delta Q = 0.615\ mm\,s^{-1}$) [12]. Values of δ and ΔQ from natural crystals [11] are included as a band in this figure for comparison purposes.

On comparing our XRD and Mössbauer data (Figs 1, 3 and 4) one must consider several relevant facts in the formation and crystallization of the pyrite

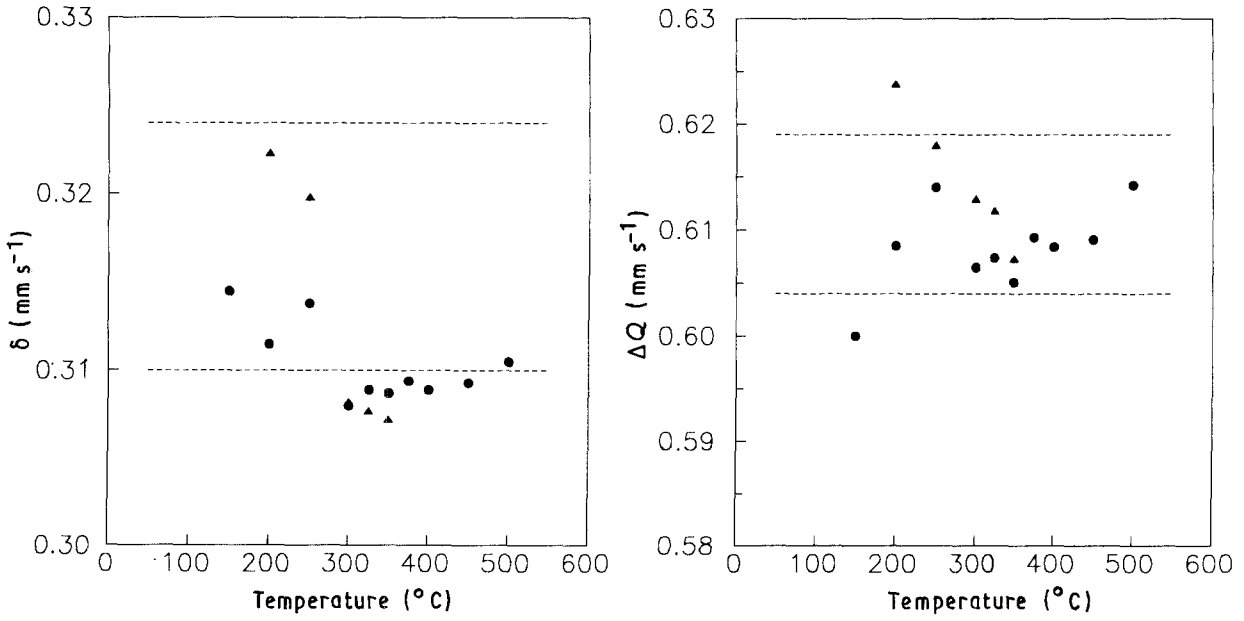

Figure 5 Mössbauer parameters of ^{57}Fe sulphidated films as a function of the temperature ($150\,^{\circ}C < T < 500\,^{\circ}C$): (●) TH, (▲) GR. Values of δ and ΔQ from natural samples [11] range between the two dashed lines drawn in the figure.

films. We have already mentioned that no XRD peaks were obtained with films sulphidated at temperatures $T < 300\,^{\circ}C$ in spite of being formed, fully or partly, by FeS_2. This means that at these sulphidation temperatures the pyrite films are amorphous or are made up of very small crystallites. Therefore the main process taking place at the lower sulphidation temperatures seems to be pyrite formation through sulphur diffusion into the Fe film. However, we cannot conclude from the results of this paper that the pyrite obtained will be stoichiometric. It probably contains sulphur vacancies whose density is reduced on increasing the sulphidation temperature. The optical absorption spectra shown below support this view. On the other hand, the pyrite film crystallization presents a more complicated behaviour: it improves on increasing the sulphidation temperature from 300 to 400 °C. This critical or singular temperature (400 °C) seems not to be related to the chemical composition of the films, in that no similar behaviour is shown either by the Mössbauer spectra or by any of the two parameters plotted in Fig. 5. Finally, the change of crystallization habit of the films sulphidated at temperatures higher than 400 °C has no parallel in the Mössbauer results.

3.3. Optical absorption

Optical absorption spectra of the films sulphidated at different temperatures are presented in Fig. 6. Optical density (OD) and not the absorption coefficient is plotted in the figure due to the different thicknesses (between ≈ 0.3 and 0.5 μm) of the films of the TH group. Several characteristics of the absorption curves change on increasing the sulphidation temperature. Firstly, the values of the absorption coefficient in the flat zone of the curves ($h\nu \approx 3$ eV) increase until they reach a maximum ($> 10^5\ cm^{-1}$) at 400 °C, which is of the order of the typical values shown by single crystals of pyrite [16]. Secondly, some structure appears in the region $2 < h\nu < 4$ eV of the first three (200–300 °C) spectra: they have two peaks at photon energies of ≈ 2.2–2.4 and 3.8–4.4 eV which can be ascribed [1, 17] to intrinsic absorption of pyrite due to band-to-band transitions. Once the absorption becomes higher ($T \geqq 350\,^{\circ}C$) this structure is not resolved. We must remark that the films obtained at 450 and 500 °C present some inhomogeneities (pinholes and so on) which tend to increase their transparency. The curves given in Fig. 6 are not corrected for any of these factors.

We must emphasize the evolution of the absorption curves in the low photon energy region (1–2 eV) on increasing the sulphidation temperature: the variation of the OD with photon energy becomes more and more abrupt until it becomes almost vertical when $T = 400\,^{\circ}C$. An improvement of the optical quality of the films is clearly produced. This fact allows us to determine appropriate values of the absorption edge of the films, E_g, by extrapolating (dashed lines in Fig. 6) the absorption curves until they cut the energy edge as previously proposed [9, 17]. Values of E_g so obtained are plotted against sulphidation temperature in Fig. 7 together with data from previous work [9] for comparison purposes. One can see from our present data that E_g sharply increases on passing from 200 to 300 °C and reaches a final value of ≈ 1.15 eV, in very good agreement with the published data from single crystals of pyrite [17, 18]. Once more we remark that the films at 450 and 500 °C present anomalous absorption curves. The temperatures at which E_g increases correspond well with the improvement of the

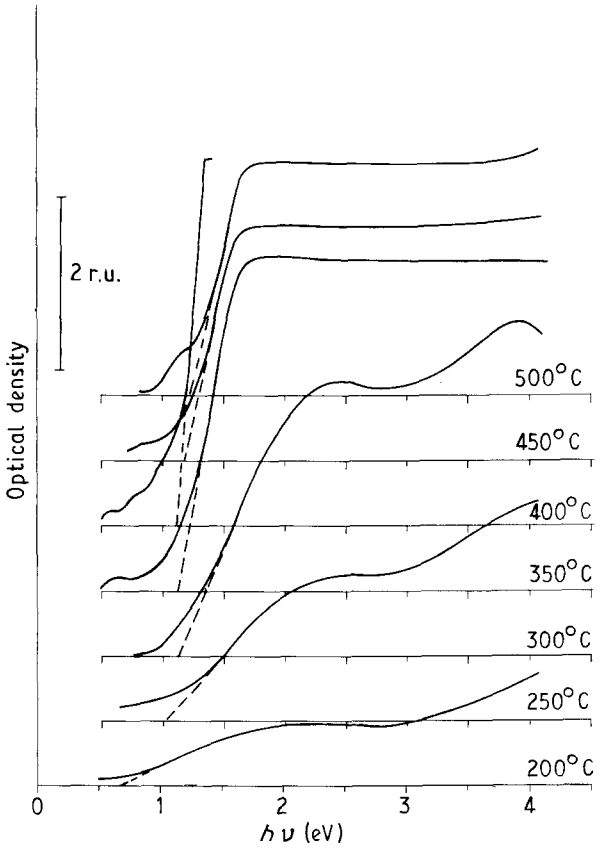

Figure 6 Optical absorption spectra at room temperature of ^{57}Fe films sulphidated at different temperatures (TH series).

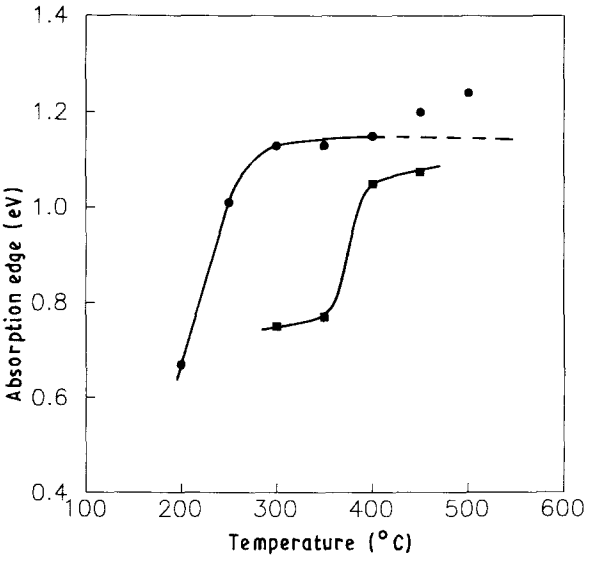

Figure 7 (●) Absorption edge, E_g, obtained from curves of Fig. 6 as a function of the sulphidation temperature of ^{57}Fe; (■) E_g values for natural Fe from previous work [9], plotted for comparison purposes (see text).

film composition as shown by the Mössbauer spectra. We therefore feel that low values of E_g (< 1.1 eV) are presented by those pyrite films with a high sulphur vacancy concentration and therefore poor stoichiometry. At $T > 300\,^{\circ}C$ the changes in the composition of the films must be small and the improvement of crystallization between 300 and 400 °C produces only a slight increase of E_g. All these suggestions are in agreement with the already published data [9, 17] and with the conclusions reached by Birkholz *et al.* [19] on discussing the possible influence of sulphur vacancies in the measured values of E_g.

Finally, comparison of the two curves of Fig. 7 evidences the important role played by the thickness of the original Fe films in the formation of the pyrite films whenever the sulphur pressure and temperature of sulphidation are the same. ^{57}Fe films used in this work were three to five times thinner than those of natural Fe used in our previous research. Due to sulphur diffusion, FeS_2 films are obtained at lower temperatures with the thinner films. At the same time, one must expect that at the same sulphidation temperature the thicker films will have a higher sulphur vacancy concentration and, therefore, will present a lower value of E_g in agreement with the experimental results of Fig. 7.

4. Conclusions

For the first time a systematic Mössbauer study of FeS_2 thin films obtained by sulphidating ^{57}Fe layers has been carried out. From this study and complementary XRD patterns and optical absorption spectra the following conclusions can be drawn.

The formation of pyrite is mainly controlled by the diffusion of sulphur into the Fe film at the sulphidation temperatures used in our research. At the lower temperatures the films are composed of Fe and pyrite and at the higher ones only pyrite is present. The films are fully converted to FeS_2 at temperatures which depend on the thickness of the initial iron film.

Crystallization of the pyrite films formed seems to improve up to sulphidation temperatures $\approx 400\,^{\circ}C$. At higher temperatures some inhomogeneities appear in the films due to a change of the crystallization habits of pyrite.

Optical properties of the films are mainly related to their composition and stoichiometry. The best values of the absorption edge, E_g, obtained are of the order of 1.15 eV and the higher absorption coefficients are $> 10^5\ cm^{-1}$. It has been proposed that the sulphur vacancy content of the films is responsible of the evolution of E_g with the sulphidation temperature.

Acknowledgements

The authors would thank F. Moreno and R. Diez for their technical support. This work was partially supported by C.A.M. (Madrid) and CICYT (Spain) under Acción Especial No. MAT91-1183-E.

References

1. K. SATO, *Prog. Cryst. Growth Charact.* **11** (1985) 109.
2. G. CHATZITHEODOROU, S. FIECHTER, M. KUNST, J. LUCK and H. TRIBUTSCH, *Mater. Res. Bull.* **231** (1988) 1261.
3. G. SMESTAD, A. DA SILVA, H. TRIBUTSCH, S. FIECHTER, M. KUNST, N. MEZIANI and M. BIRKHOLZ, *Solar Energ. Mater.* **18** (1989) 299.
4. W. JAEGERMANN and H. TRIBUTSCH, *J. Appl. Electrochem.* **13** (1983) 743.
5. A. ENNAOUI and H. TRIBUTSCH, *Solar Cells* **13** (1984) 197.
6. G. SMESTAD, A. ENNAOUI, S. FIECHTER, H. TRIBUTSCH, W. K. HOFMANN and M. BIRKHOLZ, *Solar Energ. Mater.* **20** (1990) 149.
7. C. DE LAS HERAS and C. SANCHEZ, *Thin Solid Films* **199** (1991) 259.
8. S. BAUSCH, B. SAILER, H. KEPPNER, G. WILLEKE, E. BUCHER and G. FROMMEYER, *Appl. Phys. Lett.* **57** (1990) 25.
9. I. J. FERRER and C. SANCHEZ, *J. Appl. Phys.* **70** (1991) 2641.
10. C. DE LAS HERAS, I. J. FERRER and C. SANCHEZ, *Appl. Surf. Sci.* **50** (1991) 505.
11. B. J. EVANS, R. G. JOHNSON, T. E. SENFTLE, C. BLAINE CECIL and F. DULONG, *Geochim. Cosmochim. Acta* **46** (1982) 761.
12. B. J. EVANS, H. M. KING, J. J. RENTON and A. STILLER, *Hyperfin. Int.* **57** (1990) 2187.
13. S. S. SEEHRA, P. A. MONTANO and M.S. SEEHRA, *J. Mater. Sci.* **14** (1979) 2761.
14. V. P. GUPTA, K. CHANDRA and V. K. SRIVASTAVA, *J. Mater. Sci. Lett.* **5** (1986) 165.
15. J. D. TORNERO and A. H. BRAVO, *Solid State Commun.* **61** (1987) 303.
16. A. ENNAOUI, S. FIECHTER and H. TRIBUTSCH, *J. Electrochem. Soc.* **132** (1985) 1579.
17. I. J. FERRER, D. M. NEVSKAIA, C. DE LAS HERAS and C. SANCHEZ, *Solid State Commun.* **74** (1990) 913.
18. I. J. FERRER and C. SANCHEZ, *ibid.* **81** (1992) 371.
19. M. BIRKHOLZ, S. FIECHTER, A. HARTMANN and H. TRIBUTSCH, *Phys. Rev.* **B43** (1991) 1 1926.

Received 24 September 1991
and accepted 7 April 1992